局在および細胞形態に変化は生じないことから、今後、変異ラミン A の機能解析を詳細に進めていく必要がある.

F. 健康危険情報
特になし

G. 研究発表
1. 論文発表
なし

2. 学会発表
Matsuda C, Kameyama K, Tagawa K, Ogawa M, Suzuki A, Yamaji S, Okamoto H, Nishino I, Hayashi YK. Dysferlin interacts with affixin (beta-parvin) at sarocolemma: XIth International Congress on Neuromuscular Disease. Istanbul, Turkey, July 2006.

H. **知的財産権の出願・登録状況（予定を含む）**
1. 特許取得
特になし

2. 実用新案登録
特になし

3. その他
特になし

Ⅲ.　研究成果の刊行に関する一覧表

研究成果の刊行に関する一覧表

発表者氏名： 論文タイトル名．発表誌名 巻号： ページ，出版年
Goto K, Nishino I, Hayashi YK: Rapid and accurate diagnosis of facioscapulohumeral muscular dystrophy. ***Neuromuscul Disord*** 16:256-261. 2006.
Taniguchi M, Kurahashi H, Noguchi S, Fukudome T, Okinaga T, Tsukahara T, Tajima Y, Ozono K, Nishino I, Nonaka I, Toda T: Aberrant neuromuscular junctions and delayed terminal muscle fiber maturation in α-dystroglycanopathies. ***Hum Mol Genet*** 15:1279-1289. 2006.
Wu S, Ibarra MCA, Malicdan MCV, Murayama K, Ichihara Y, Kikuchi H, Nonaka I, Noguchi S, Hayashi YK, Nishino I: Central core disease is due to RYR1 mutations in more than 90% of patients. ***Brain*** 129: 1470-1480, 2006.
Malicdan MC, Noguchi S, Nonaka I, Hayashi YK, Nishino I: A Gne knockout mouse expressing human V572L mutation develops features similar to distal myopathy with rimmed vacuoles or hereditary inclusion body myopathy. ***Hum Mol Genet*** 16: 115-128, 2007.
Osawa M, Liewluck T, Ogata K, Iizuka T, Hayashi YK, Nonaka I, Sasaki M, Nishino I: Familial reducing body myopathy. ***Brain Dev*** 29: 112-116, 2007.
Liewluck T, Hayashi YK, Osawa M, Kurokawa R, Fujita M, Noguchi S, Nonaka I, Nishino I: Unfolded protein response and aggresome formation in hereditary reducing body myopathy. ***Muscle Nerve*** 35:322-326, 2007.
Keira Y, Noguchi S, Kurokawa R, Fujita M, Minami N, Hayashi YK, Kato T, Nishino I: Characterization of lobulated fibers in limb girdle muscular dystrophy type 2A by gene expression profiling. ***Neurosci Res*** 57:513-521, 2007.

Ⅳ.　研究成果の刊行物・別刷

PERGAMON

Neuromuscular Disorders 16 (2006) 256–261

www.elsevier.com/locate/nmd

Rapid and accurate diagnosis of facioscapulohumeral muscular dystrophy

Kanako Goto, Ichizo Nishino, Yukiko K. Hayashi *

Department of Neuromuscular Research, National Institute of Neuroscience, National Center of Neurology and Psychiatry (NCNP), 4-1-1 Ogawa-Higashi, Kodaira, Tokyo 187-8502, Japan

Received 10 September 2005; received in revised form 9 January 2006; accepted 18 January 2006

Abstract

Facioscapulohumeral muscular dystrophy (FSHD) is a common muscular disorder, but clinical and genetic complications make its diagnosis difficult. Southern blot analysis detects a smaller sized *Eco*RI fragment on chromosome 4q35 in most facioscapulohumeral muscular dystrophy patients, that contains integral number of 3.3-kb tandem repeats known as D4Z4. The problems for the genetic diagnosis are that southern blotting for facioscapulohumeral muscular dystrophy is quite laborious and time-consuming, and the D4Z4 number is only estimated from the size of the fragment. We developed a more simplified diagnostic method using a long polymerase chain reaction (PCR) amplification technique. Successful amplification was achieved in all facioscapulohumeral muscular dystrophy patients with an *Eco*RI fragment size ranging from 10 to 25 kb, and each patient had a specific polymerase chain reaction product which corresponded to the size calculated from the number of D4Z4. Using southern blot analysis, more than 90% of facioscapulohumeral muscular dystrophy patients have a smaller *Eco*RI fragment than 26 kb in our series, and the number of D4Z4 repeats is precisely counted by this polymerase chain reaction method. We conclude that this long polymerase chain reaction method can be used as an accurate genetic screening technique for facioscapulohumeral muscular dystrophy patients.

Keywords: Facioscapulohumeral muscular dystrophy; Chromosome 4q35; Genetic diagnosis; Southern blotting; PCR; *Eco*RI fragment; D4Z4

1. Introduction

Facioscapulohumeral muscular dystrophy (FSHD) is a common autosomal dominant muscular disorder characterized by its distinct clinical presentation. It often involves weakness and atrophy of facial muscles, followed by shoulder-girdle, the scapula fixators, and the upper arm muscles. Subsequently, pelvic girdle and lower limbs are also affected. About 20% of the patients eventually become wheelchair-bound by 40 years of age [1]. Difficulties of whistling, eye closure, or arm raising are common initial symptoms. Prominent scapular winging and horizontally positioned clavicles are also observed. Facial or shoulder girdle weakness usually appears during adolescence, but signs may be apparent on examination even in early childhood. Asymmetry of muscle involvement is often observed in apparently affected patients, but this is unrelated to handedness [2]. Weakness is relatively mild and the progression is usually slow with frequent association of subclinical hearing loss and retinal vasculopathy. The clinical diagnosis of FSHD is sometimes difficult because the onset of illness and the phenotypic expression is extremely variable, both within and between families [3,4].

The gene locus for FSHD has been identified on chromosome 4q35 wherein an array of tandem repeat units is located. Each repeat is a 3.3-kb *Kpn*I digestable fragment designated as D4Z4 (Fig. 1) [5–7]. The disease is usually associated with a deletion of this repeated region, however the responsible gene has not yet been identified, and the underlying molecular mechanism is still enigmatic. Southern blot analysis using the probe p13E-11 (D4F104S1) [6] is usually performed in the genetic diagnosis of FSHD. Normal individuals have *Eco*RI digested fragments containing D4Z4 repeats which varies from 40 kb to more than 300 kb in size, however, most of the FSHD patients have a smaller sized fragment from 10 to 35 kb. The clinical severity is often correlated to the fragment size, and patients with the smallest *Eco*RI fragment show very early onset and can be associated with epilepsy and mental retardation [8,9].

* Corresponding author. Tel.: +81 42 341 2712; fax: +81 42 346 1742.
E-mail address: hayasi_y@ncnp.go.jp (Y.K. Hayashi).

0960-8966/$ - see front matter © 2006 Elsevier B.V. All rights reserved.
doi:10.1016/j.nmd.2006.01.008

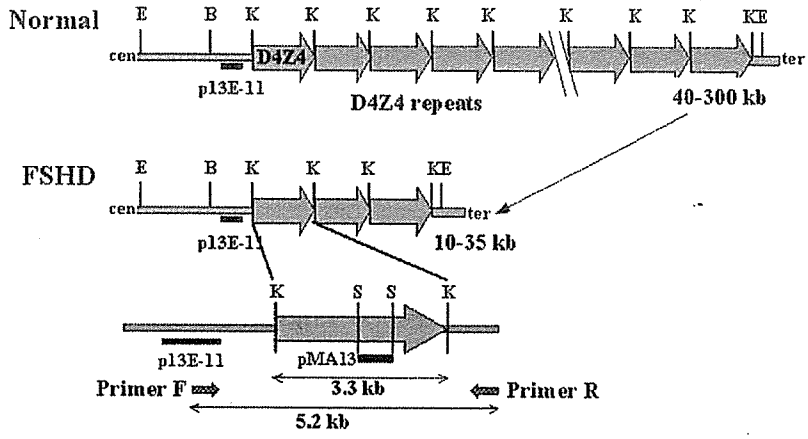

Fig. 1. A schematic diagram of the FSHD gene region on chromosome 4q35 showing the relative locations of primers and the probes used in this study. The primer set has been designed in the non-repeated region, and is expected to produce a 5.2 kb PCR amplified product when template genomic DNA contains one D4Z4 repeat. Cen, centromeric side of the gene; ter, telomeric side of gene; E, *Eco*RI; B, *Bln*I; K, *Kpn*I; S, *Sal*I.

Presently, the accuracy of the molecular diagnosis for FHSD using southern blot is up to 98% [10], however, several factors make this method cumbersome, and more than a week-length of time is required to obtain the results. In the conventional southern blotting method, it is difficult to resolve fragment size over 50 kb, and pulsed-field gel electrophoresis (PFGE) is sometimes taken together to increase resolution. Somatic and germline mosaicism is frequently observed in which more than three different sized *Eco*RI fragments on chromosome 4q are identified [11,12]. Furthermore, homologous 3.3-kb repeat-like sequences are also identified on many other chromosomes such as chromosomes Y and 3p [13,14]. In addition, chromosome 10q26 also contains 3.3-kb *Kpn*I digestable tandem repeats with 98% nucleotide identity to D4Z4 on chromosome 4 [15,16]. Consequently, there is a high incidence of inter-chromosomal exchange between 4q35 and 10q26, which is observed in about 20% of normal individuals [17,18]. In southern blot analysis, the probe p13E-11 used is not specific only to recognize *Eco*RI fragment from chromosome 4q but can also identify *Eco*RI fragment on chromosomes 10q26 and Y. This would require double restriction enzyme digestion using *Eco*RI and *Bln*I to be performed to distinguish 4q35-derived D4Z4 (*Bln*I-resistant) from 10q26-derived repeated units (*Bln*I-sensitive) [19]. From these complexities, there is an urgent need to develop a more simplified and reliable method for the diagnosis of FSHD.

Here, we introduce a new method to count the numbers of D4Z4 repeats on chromosome 4q35 by using long PCR amplification, which is quite useful for the rapid and accurate genetic diagnosis of FSHD.

2. Materials and methods

All clinical materials used in this study were acquired with informed consent. One hundred and five patients with a 4q-linked small *Eco*RI fragment from 10 to 35 kb (Table 3), and seven healthy individuals were examined. Genomic DNA was carefully and gently extracted from blood lymphocytes using a standard method. Southern blot analysis using the probe p13E-11 was performed as previously described [12].

For a long PCR amplification, a 50 μl reaction mixture was used. This mixture contains 400–600 ng of genomic DNA, 25 μl of 2× GC Buffer I (TAKARA BIO INC. Japan), 7.5 μl dATP/dTTP/dCTP mixture (10 mM each), 2.5 μl dGTP/7-deaza-dGTP mix (2:3), 1 μl (10 pM/μl) of each primers, and 0.5 μl (5 U/μl) LA Taq HS (TAKARA BIO). The primers were designed based on the human genomic sequences from GenBank (Accession Numbers D38025 and U74497). The primer sequences are F: 3′-GGCCAGAGTTT-GAATATACTGTGGTCATCTCTGCTCCAG-5′, R: 3′-CAGGGGATATTGTGACATATCTCTGCACTCATC. Amplification was performed using GeneAmp PCR System 9700 (PerkinElmer Japan Co., Ltd, Japan) with the following conditions; 1 min at 94 °C for the initial denaturation, followed by 10 cycles of 10 s at 98 °C and 20 min at 64 °C, and an additional 23 cycles of 10 s at 98 °C, 20 min with autoextension of 20 s per cycle at 64 °C, and 10 min at 72 °C for final elongation. The PCR products were separated by electrophoresis using 0.4% SeaKem HGT agarose gel (FMC BioProducts, ME) in 1× TAE with 0.5 μg/ml ethidium bromide at 3 h. High Molecular Weight DNA Marker (8.3–48.5 kb) (Invitrogen Japan K.K., Japan) and 1 kb plus ladder (Invitrogen) were used. The number of the 3.3 kb *Kpn*I repeated units in the FSHD gene region was calculated by the sequence data from GenBank (Accession Numbers D38024, D38025, and U74497).

In order to ascertain the specificity of the amplified products, we transferred the gels to Hybond N^+ (Amersham Biosciences, Japan) and overnight hybridization at 65 °C was performed with the ^{32}P-labeled probes of p13E-11 and pMA13 (1.3 kb *Stu*I fragment within a D4Z4 unit). The membrane was washed in a stringency of 2× SSC/0.1% SDS for 20 min at 65 °C for two times, followed by

Table 1
Comparison of long PCR and southern blot (SB) analyses

	PCR	SB
Template DNA (μg)	0.4	40
Enzyme digestion	No	*Eco*RI, *Bln*I
Gel size, concentration	11×14 cm, 0.4%	20×20 cm, 0.3%
Required time (h)		
PCR	11	0
Electrophoresis	3	68
Transfer	0	18
Hybridization	0	18
Detection	EB	RI
Total time required	<1 day	7–10 days
Accuracy (%)	90.1[a]	98 [10]

EB, ethidium bromide; RI, radio isotope.
[a] Estimated from the distribution of *Eco*RI fragment size in our series as described in Table 2.

autoradiography for 2 h using BAS2500 image analyzer (Fiji Photo Film, Japan).

3. Results

Table 1 shows the comparison of our newly developed long PCR method and the conventional southern blot analysis. This long PCR method is quite simple, requiring only a small amount of genomic DNA (1/100 of the quantity for southern blotting) and results are rapidly acquired overnight.

The long PCR method amplified five different sized products of 5.2, 8.5, 11.8, 15.1 and 18.4 kb which corresponded to the calculated size from the sequence data of the FSHD region containing one to five D4Z4 repeats, respectively (Fig. 2a, Table 3). These PCR products were not digested by *Bln*I, and were exclusively hybridized by the two probes of p13E-11 and pMA13 (data not shown). The same PCR method was performed on 10 individuals with a small *Eco*RI fragment (from 10 to 25 kb) on chromosome 10q26 but no amplified product was identified (data not shown).

Table 2 shows the distribution of the size of small *Eco*RI fragment on chromosome 4q of 263 FSHD families in our series. Table 3 shows the size of the PCR products, the calculated size of the *Eco*RI fragment, the range of the fragment size detected by southern blot analysis, and number of the patients. A 5.2 kb PCR product that contains one D4Z4 repeat was observed in eight patients with a *Eco*RI fragment from 10 to 11 kb. Sequence analysis confirmed that this 5.2 kb fragment contains one D4Z4 repeat on chromosome 4q35. An 8.5 kb band corresponding to the size with two D4Z4 repeated units was detected in 23 patients with 13–17 kb *Eco*RI fragment. An 11.8 kb product (three D4Z4 repeats) was seen in 26 patients with 16–19 kb fragment, a 15.1 kb fragment (four D4Z4 repeats) was seen in 24 patients with 18–22 kb fragment, and a 18.4 kb product (five D4Z4 repeats) was observed in six patients with 23–25 kb *Eco*RI fragment. The PCR products were amplified from all 87 DNA samples of the patients with an *Eco*RI fragment of 25 kb or less. However, DNA from normal individuals and FSHD patients with larger (≧26 kb) *Eco*RI fragments were not successfully amplified/detected by this long PCR method.

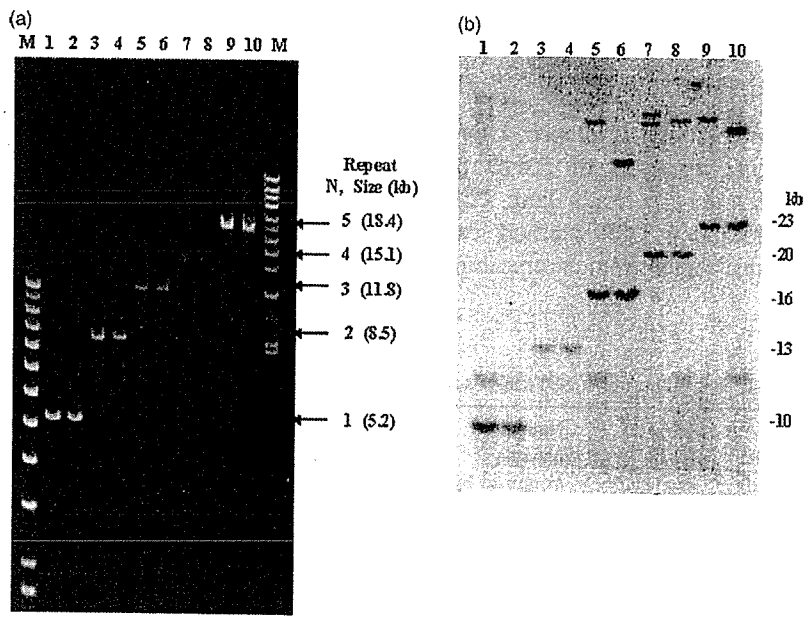

Fig. 2. Long PCR amplification and conventional southern blot analysis using genomic DNA from FHSD patients. (a) A 5.2 kb PCR product was detected on two patients with an *Eco*RI fragment of 10-kb (lane 1), or 11-kb (lane 2) as interpreted from our previous southern blot study. An 8.5-kb band was detected from two patients with a 13-kb (lane 3) or a 14-kb (lane 4) fragment, an 11.8-kb product from two patients with a 16-kb (lane 6) or a 17-kb (lane 7) fragment, a 15.1-kb product from a 20 or a 22 kb fragment, and an 18.4 kb fragment was identified from patients with a 24 and a 25 kb *Eco*RI fragment. These PCR products correspond to the size containing one to five D4Z4 repeated units. (b) Southern blot analysis using the same 10 samples in (a). The samples with the same size of the PCR products showed no difference of the *Eco*RI fragment size, although variable fragment size was previously interpreted.

Table 2
Distribution of *Eco*RI fragment size on chromosome 4q of 263 families in our series

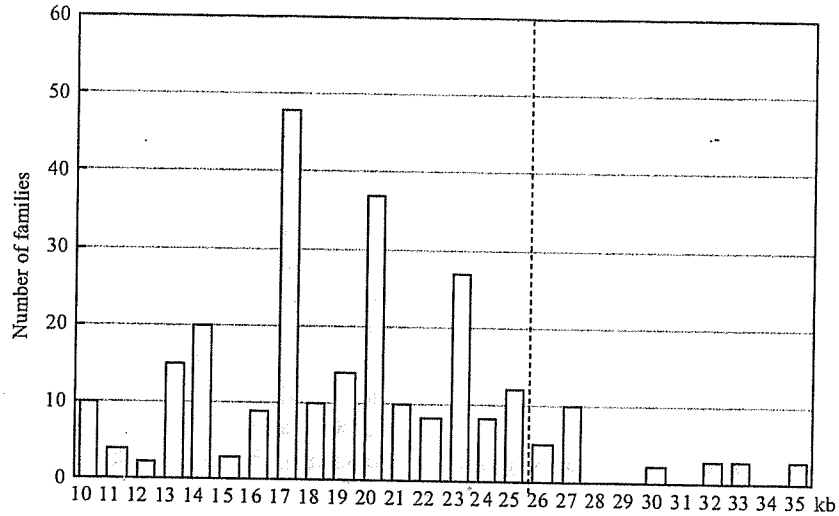

*Eco*RI fragments of <26 kb (dot line) can be amplified by long PCR analysis.

Estimated fragment size from the previous southern blot was not identical among the patients with same numbers of D4Z4 repeats. To determine the inter-individual variability of the fragment size, conventional southern blot analysis was repeated simultaneously. Notably, after the repeated southern blot technique, the *Eco*RI fragment size was similar when the D4Z4 number was the same and this result was consistent with the calculated size (Fig. 2b).

4. Discussions

In this study, we have successfully developed a new method for rapid and specific diagnosis of FSHD by counting the number of D4Z4 repeats via a long PCR amplification technique. This long PCR method can specifically amplify the repeated region from chromosome 4q up to 18.4 kb in size and countable from one to five D4Z4 repeated units.

Table 3
Comparison of the results of long PCR and southern blot (SB) analysis

Number of D4Z4 repeats	PCR product size (kb)	Calculated size of *Eco*RI fragment (kb)	Range of *Eco*RI fragment by SB (kb)	Number of patients examined by PCR
1	5.2	10.2	10-11	8
2	8.5	13.5	13–17	23
3	11.8	16.8	16–19	26
4	15.1	20.1	18–22	24
5	18.4	23.4	23–25	6
6	21.7	26.7	26–35	18 (No amplification)
7	25	30		
8	28.3	33.3		
9	31.6	36.6		

D4Z4 repeat has highly GC-rich sequence up to 73% [20]. Difficulties in PCR amplification often arise when GC content of the template DNA exceeds 50%. This difficulty in PCR amplification was overcame in our study by using thermo-stable long accurate Taq, 7-deaza-dGTP, and a higher denaturing temperature (98 °C) followed by a relatively higher annealing/extension temperature (64 °C) for 20 min with autoextension of 20 s per cycle. Therefore 73% of GC-containing repeated region of more than 18 kb in size was amplified with ease. The specificity of each PCR amplified product was ascertained by several ways. First, both probes (p13E-11 and pMA-13) that were used in the hybridization of the PCR products exclusively recognize fragments containing D4Z4 repeats. Second, the restriction enzyme *Bln*I did not digest the amplified fragments and confirmed that the product is apparently different from the repeats derived from chromosome 10q26, wherein 98% homologous *Kpn*I repeated units and franking sequences are known. Third, this long PCR method did not amplify *Kpn*I repeats from 10q26 even though the only difference is one different nucleotide from each of the primer region on 4q35. We also designed 10q-specific primer set and confirmed that only the 10q-derived repeats could be amplified by using this primer set.

The diagnosis of FSHD is sometimes difficult. Clinical symptoms and severity are quite variable between the patients even within the same family. Up to date, genetic diagnosis of FSHD is solely depended on the southern blot analysis since no responsible gene is yet identified within the candidate region. However, such procedure requires a large amount of DNA and would necessitate at least a week-time period to produce results. The requirement for such

amount of time for analysis dwells on the complexity of the experimental protocols in detecting the various fragments, the sizes ranging from 10 to 300 kb, as well as the determination of the existence of homologous regions on the other chromosomes. Determination of the size of *Eco*RI fragment is important since it is usually correlated to the clinical severity. However, identification of the precise fragment size is often difficult in the conventional southern blotting, since only very low concentrated gels of 0.3% is used to detect large sized fragment, and even minor changes in the experimental conditions would produce different results. In fact, in our very own series, DNA samples containing the same number of D4Z4 repeats showed the same *Eco*RI fragment size on one membrane although the estimated size in our previous analysis detected by different membranes were variable. Therefore, the number of D4Z4 units estimated from the *Eco*RI fragment size using Southern blotting could be misinterpreted from its actual number. From the result of the long PCR analysis, we concluded that the number of D4Z4 is countable from the size of PCR products, and the deletion of the FSHD region is certainly caused by the deleted integral number of D4Z4.

The number of D4Z4 is specifically countable up to five, which corresponds to the estimated *Eco*RI fragment of 10–25 kb in size. When no amplified product was obtained, southern blot analysis is required. In our series, 9.9% of the 4q-linked small *Eco*RI fragments have 26–35 kb as shown in Table 2, but the percentage may be greater in other countries. In the cases having deletion of p13E-11, no product can be obtained in this PCR analysis, since the forward primer is designed within this region. However, considering the complexity of the southern blot technique, this long PCR analysis is useful for the initial screening of the FSHD patients, and also the genetic test for the other family members with a known D4Z4 repeat numbers from 1 to 5 in an index patient. Obtaining accurate results rapidly is always beneficial for the patient, especially during prenatal test. From the economical point of view, PCR analysis is also beneficial since it costs 1/30–40 for the southern blot analysis.

Both primer sequences we used in this study are 4q-specific, and can amplify fragments even those with zero D4Z4 repeat, if any, producing an estimated 1.9-kb product. We also designed a primer set that can specifically amplify the repeated region on chromosome 10q. Theoretically, by using several combinations of these primers, we should be able to distinguish rare cases with short hybrid repeats on 4q or non-FSHD *Bln*I-resistant fragments on 10q. We concluded that the long PCR method could be used as an accurate genetic screening technique for FSHD.

Acknowledgements

We would like to thank Dr Mina Nolasco Astejada (NCNP) for critically reviewing the manuscript. This work was supported by Health and Labor Science Research Grants, Research on Psychiatric and Neurological Diseases and Mental Health, and The Research Grant (17A-10) for Nervous and Mental Disorders from the Ministry of Health, Labour and Welfare, Research on Health Sciences focusing on Drug Innovation from The Japan Health Sciences Foundation, Japan.

References

[1] Lunt PW, Harper PS. Genetic counselling in facioscapulohumeral muscular dystrophy. J Med Genet 1991;28:655–64.
[2] Tawil R, McDermott MP, Mendell JR, Kissel J, Griggs RC. Facioscapulohumeral muscular dystrophy (FSHD): design of natural history study and results of baseline testing, FSH-DY group. Neurology 1994;44:442–6.
[3] Lunt PW, Jardine PE, Koch M, et al. Phenotypic–genotypic correlation will assist genetic counseling in 4q35-facioscapulohumeral muscular dystrophy. Muscle Nerve 1995;2:S103–S9.
[4] Padberg GW, Frants RR, Brouwer OF, Wijmenga C, Bakker E, Sandkuijl LA. Facioscapulohumeral muscular dystrophy in the Dutch population. Muscle Nerve 1995;2:S81–S4.
[5] Upadhyaya M, Lunt P, Sarfarazi M, Broadhead W, Farnham J, Harper PS. The mapping of chromosome 4q markers in relation to facioscapulohumeral muscular dystrophy (FSHD). Am J Hum Genet 1992;51:404–10.
[6] Wijmenga C, Hewitt JE, Sandkuijl LA, et al. Chromosome 4q DNA rearrangements associated with facioscapulohumeral muscular dystrophy. Nat Genet 1992;2:26–30.
[7] Hewitt JE, Lyle R, Clark LN, et al. Analysis of the tandem repeat locus D4Z4 associated with facioscapulohumeral muscular dystrophy. Hum Mol Genet 1994;3:1287–95.
[8] Funakoshi M, Goto K, Arahata K. Epilepsy and mental retardation in a subset of early onset 4q35-facioscapulohumeral muscular dystrophy. Neurology 1998;50:1791–4.
[9] Miura K, Kumagai T, Matsumoto A, et al. Two cases of chromosome 4q35-linked early onset facioscapulohumeral muscular dystrophy with mental retardation and epilepsy. Neuropediatrics 1998;29: 239–41.
[10] Upadhyaya M, Cooper DN. Molecular diagnosis of facioscapulohumeral muscular dystrophy. Expert Rev Mol Diagn 2002;2: 160–71.
[11] Lemmers RJ, van der Wielen MJ, Bakker E, Padberg GW, Frants RR, van der Maarel SM. Somatic mosaicism in FSHD often goes undetected. Ann Neurol 2004;55:845–50.
[12] Goto K, Nishino I, Hayashi YK. Very low penetrance in 85 Japanese families with facioscapulohumeral muscular dystrophy 1A. J Med Genet 2004;41:e12.
[13] Clark LN, Koehler U, Ward DC, Wienberg J, Hewitt JE. Analysis of the organisation and localisation of the FSHD-associated tandem array in primates: implications for the origin and evolution of the 3.3 kb repeat family. Chromosoma 1996; 105:180–9.
[14] Ballarati L, Piccini I, Carbone L, et al. Human genome dispersal and evolution of 4q35 duplications and interspersed LSau repeats. Gene 2002;296:21–7.
[15] Deidda G, Cacurri S, Grisanti P, Vigneti E, Piazzo N, Felicetti L. Physical mapping evidence for a duplicated region on chromosome 10qter showing high homology with the facioscapulohumeral muscular dystrophy locus on chromosome 4qter. Eur J Hum Genet 1995;3:155–67.

[16] van Geel M, Dickson MC, Beck AF, et al. Genomic analysis of human chromosome 10q and 4q telomeres suggests a common origin. Genomics 2002;79:210–7.
[17] Matsumura T, Goto K, Yamanaka G, et al. Chromosome 4q;10q translocations; comparison with different ethnic populations and FSHD patients. BMC Neurol 2002;2:7.
[18] Lemmers RJ, van der Maarel SM, van Deutekom JC, et al. Inter- and intrachromosomal sub-telomeric rearrangements on 4q35: implications for facioscapulohumeral muscular dystrophy (FSHD) aetiology and diagnosis. Hum Mol Genet 1998;7: 1207–14.
[19] Deidda G, Cacurri S, Piazzo N, Felicetti L. Direct detection of 4q35 rearrangements implicated in facioscapulohumeral muscular dystrophy (FSHD). J Med Genet 1996;33:361–5.
[20] Lee JH, Goto K, Matsuda C, Arahata K. Characterization of a tandemly repeated 3.3-kb KpnI unit in the facioscapulohumeral muscular dystrophy (FSHD) gene region on chromosome 4q35. Muscle Nerve 1995;2:S6–S13.

Human Molecular Genetics, 2006, Vol. 15, No. 8 *1279–1289*
doi:10.1093/hmg/ddl045
Advance Access published on March 10, 2006

Aberrant neuromuscular junctions and delayed terminal muscle fiber maturation in α-dystroglycanopathies

Mariko Taniguchi[1], Hiroki Kurahashi[3], Satoru Noguchi[4], Takayasu Fukudome[5], Takeshi Okinaga[2], Toshifumi Tsukahara[6], Youichi Tajima[7], Keiichi Ozono[2], Ichizo Nishino[4], Ikuya Nonaka[4] and Tatsushi Toda[1,*]

[1]Division of Clinical Genetics, Department of Medical Genetics and [2]Department of Pediatrics, Osaka University Graduate School of Medicine, 2-2 Yamadaoka, Suita, Osaka 565-0871, Japan, [3]Division of Molecular Genetics, Institute for Comprehensive Medical Science, Fujita Health University, Toyoake, Aichi 470-1192, Japan, [4]National Institute of Neuroscience, National Center of Neurology and Psychiatry, Kodaira, Tokyo 187-8502, Japan, [5]Division of Clinical Research, Nagasaki Medical Center of Neurology, Kawatanamachi, Nagasaki 859-3615, Japan, [6]Center for Nano Materials and Technology, Japan Advanced Institute of Science and Technology, Tatsunokuchi, Ishikawa 923-1292, Japan and [7]Department of Clinical Genetics, The Tokyo Metropolitan Institute of Medical Science, Bunkyo-ku, Tokyo 113-8613, Japan

Received October 15, 2005; Revised and Accepted February 28, 2006

Recent studies have revealed an association between post-translational modification of α-dystroglycan (α-DG) and certain congenital muscular dystrophies known as secondary α-dystroglycanopathies (α-DGpathies). Fukuyama-type congenital muscular dystrophy (FCMD) is classified as a secondary α-DGpathy because the responsible gene, *fukutin*, is a putative glycosyltransferase for α-DG. To investigate the pathophysiology of secondary α-DGpathies, we profiled gene expression in skeletal muscle from FCMD patients. cDNA microarray analysis and quantitative real-time polymerase chain reaction showed that expression of developmentally regulated genes, including myosin heavy chain (*MYH*) and myogenic transcription factors (*MRF4*, *myogenin* and *MyoD*), in FCMD muscle fibers is inconsistent with dystrophy and active muscle regeneration, instead more of implicating maturational arrest. FCMD skeletal muscle contained mainly immature type 2C fibers positive for immature-type MYH. These characteristics are distinct from Duchenne muscular dystrophy, suggesting that another mechanism in addition to dystrophy accounts for the FCMD skeletal muscle lesion. Immunohistochemical analysis revealed morphologically aberrant neuromuscular junctions (NMJs) lacking MRF4 co-localization. Hypoglycosylated α-DG indicated a lack of aggregation, and acetylcholine receptor (AChR) clustering was compromised in FCMD and the myodystrophy mouse, another model of secondary α-DGpathy. Electron microscopy showed aberrant NMJs and neural terminals, as well as myotubes with maturational defects. Functional analysis of NMJs of α-DGpathy showed decreased miniature endplate potential and higher sensitivities to *d*-Tubocurarine, suggesting aberrant or collapsed formation of NMJs. Because α-DG aggregation and subsequent clustering of AChR are crucial for NMJ formation, hypoglycosylation of α-DG results in aberrant NMJ formation and delayed muscle terminal maturation in secondary α-DGpathies. Although severe necrotic degeneration or wasting of skeletal muscle fibers is the main cause of congenital muscular dystrophies, maturational delay of muscle fibers also underlies the etiology of secondary α-DGpathies.

* To whom correspondence should be addressed. Tel: +81 668793380; Fax: +81 668793389; Email: toda@clgene.med.osaka-u.ac.jp

INTRODUCTION

Fukuyama-type congenital muscular dystrophy (FCMD; MIM 253800) is an autosomal recessive muscular dystrophy and the second most common childhood muscular dystrophy in Japan, following Duchenne muscular dystrophy (DMD) (1). Clinical manifestations of FCMD include severe congenital muscular dystrophy from early infancy, cobblestone lissencephaly and eye malformation. We previously isolated the responsible gene for FCMD, termed *fukutin* (2,3). Recently, it has been postulated that *fukutin* modulates the glycosylation of α-dystroglycan (α-DG), a major component of the dystrophin–glycoprotein complex (4,5). FCMD is classified as one of the congenital muscular dystrophies, such as laminin-α2-deficient congenital muscular dystrophy (MDC1A) (6). Recently, FCMD has also been classified as a secondary α-DGpathy, as mutations in genes encoding glycosyltransferases result in hypoglycosylated α-DG (7). α-Dystroglycan binds to extracellular matrix proteins such as laminin, agrin and perlecan, which are important in maintaining muscle cell integrity (8). Hypoglycosylated α-DG provokes the post-translational disruption of dystroglycan–ligand interactions in the skeletal muscle of patients, leading to the severe phenotypes of congenital muscular dystrophies (7). Other glycosyltransferases include POMGnT1 (protein *O*-mannose β-1, 2-*N*-acetylglucosaminyltransferase 1), POMT1 and POMT2 (protein *O*-mannosyltransferases 1 and 2), fukutin-related protein (FKRP) and LARGE; mutations in these genes induce human muscle–eye–brain disease, Walker–Warburg syndrome and congenital muscular dystrophy type 1C/1D, and mouse myodystrophy, respectively (9–14).

Primary characteristics of the so-called 'muscular dystrophy' such as DMD include necrotic change and active regeneration of muscle fibers. From infancy, DMD patients usually show dystrophic change in skeletal muscle, accompanied by elevation of serum creatine kinase (CK) levels. However, DMD patients usually maintain their gait until early adolescence. In contrast, FCMD patients show severe phenotypic characteristics from very early infancy, and few patients can acquire gait regardless of serum CK levels (1). Skeletal muscle fibers in FCMD are extremely small, irregular in cell size and architecturally disorganized, and extensive fibrosis prevails from the early infantile stage. However, only a small number of muscle fibers show severe necrotic change or active myofibril regeneration, and satellite cells are also fewer than those of DMD (1,15,16). These phenotypic differences promote the hypothesis that another mechanism may also account for the pathophysiology of secondary α-DGpathies.

Although expression profiling of skeletal muscle from patients with DMD, MDC1A and α-sarcoglycanopathy have been described (17–19), no similar analysis has been reported for FCMD and other secondary α-DGpathies. To investigate the molecular mechanism of FCMD and other secondary α-DGpathies, we profiled gene expression in FCMD skeletal muscle using cDNA microarray and subsequent quantitative real-time polymerase chain reaction (PCR). Here we demonstrate that aberrant neuromuscular junctions (NMJs) and maturational delay of muscle fibers are significant to the mechanism underlying secondary α-DGpathies.

RESULTS

Aberrant muscle regeneration is suggested by gene expression profiling of FCMD skeletal muscle

Gene expression profiling of FCMD skeletal muscle was performed using a custom cDNA microarray. Clustering analysis showed similar overall expression profiles of muscle from four FCMD patients, aged 20 days to 1 year, 6 months (Fig. 1A). This similarity is independent of age and histology of the muscle specimen in our samples.

We analyzed individual genes showing distinct expression patterns in FCMD skeletal muscle compared with normal children or DMD patients. Most genes encoding muscle components were down-regulated in FCMD. Among these, *myosin light chain 1, 3* and *4* (*myl1, 3* and *4*) were up-regulated in DMD skeletal muscle, in contrast with FCMD (Fig. 1B). Expression of the developmentally regulated myosin heavy chains (*MYHs*), *MYH1*, *MYH2* and *MYH7* (slow, adult-type), was down-regulated in FCMD but not in DMD, whereas expression of *MYH8* (fast-type) showed no significant change in FCMD compared with DMD or normal controls. Slow-type MYHs (MYH1, MYH2 and MYH7) are present in mature muscle fibers and crucial for sarcomere assembly to maintain muscle integrity, whereas fast-type or developmental MYHs (MYH3, MYH4 and MYH8) are seen in early immature myoblasts or in regenerating fibers. These observations suggest that expression of mature muscle components is suppressed in FCMD skeletal muscle at all ages examined.

With regard to muscle fiber differentiation, myogenic factors including *MyoD*, *myf5* and *myogenin* (*myf4*) showed insufficient signal for the analysis. It is noteworthy, however, that *MRF4* (*myf6*) was down-regulated in FCMD. Expression of the alpha-type cholinergic receptor (*CHRNA*), which is known to be regulated by *MyoD* and *MRF4* (20,21), was much higher in FCMD patients than in normal controls.

We next performed real-time quantitative PCR to further investigate skeletal muscle differentiation. We compared mRNA expression in FCMD muscle with normal or DMD skeletal muscle, as DMD is a good example for active regeneration, in which expression of muscle component and myogenic factor mRNA expression is expected to be up-regulated. Although *CHNRA* was up-regulated in DMD, as predicted, its expression was even higher in FCMD (Fig. 2A and B). Among these cholinergic receptor subtypes, gamma-type cholinergic receptor (*CHNRG*), which is a component of fetal isoforms, was up-regulated, whereas epsilon-type cholinergic receptor (*CHNRE*), which only composes adult isoforms (22), was down-regulated in FCMD (Fig. 2B). MYH slow-type (*MYH7*) was down-regulated in FCMD, consistent with the microarray analysis, whereas expression of fast-type MYH (*MYH8/b*) was not altered in FCMD. Interestingly, although *MyoD* and *myogenin* were up-regulated in both DMD and FCMD, *MRF4* was down-regulated in FCMD muscle but up-regulated in DMD (Fig. 2A and B). *MRF4* expression is known to be up-regulated in the late phase of muscle regeneration or differentiation, followed by sequential expression of *MyoD*, *myf5* and *myogenin*, indicating significant roles in terminal differentiation (20,21). These results suggest that FCMD skeletal muscle undergoes an unbalanced differentiation process.

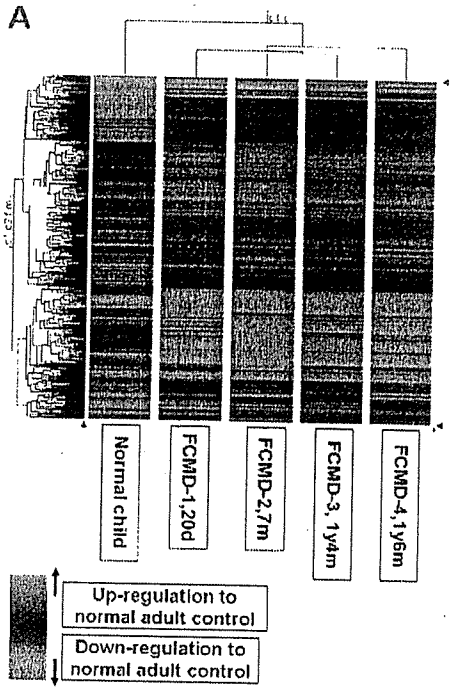

B

gene	FCMD	DMD	Product
myl1	↓	→	myosin light chain 1
myl2	↓	↑	myosin light chain 2
myl3	↓	↑	myosin light chain 3
myl4	↓	↑	atrial /embryonic alkali myosin light chain
myh1	↓↓	↑	myosin, heavy polypeptide 1, adult (slow)
myh2	↓↓	↑	myosin, heavy polypeptide 2, adult (slow)
myh7	↓↓	↑	myosin, heavy polypeptide 7, beta (slow)
myh8	↓	→	myosin, heavy polypeptide 8, (fast)
mybpc1	↓↓	↑	myosin binding protein C, slow type
mybph	↑	→	myosin-binding protein H
actc	↑	↑	actin, alpha, cardiac muscle precursor
actg1	↓	↑	actin, gamma 1
actg2	↓	↑↑	actin, gamma 2
sgcb	↓↓	↓	sarcoglycan, beta
tcap	↓↓	→	titin-cap (telethonin)
ttn	↓↓	↓	titin
des	↓↓	↑	desmin
myf6	↓	→	MRF4 (myf6,herculin)
CHRNA	↑↑	→	nicotinic type, acetylcholine receptor

Figure 1. Cluster image and gene trees from expression profiling of FCMD and normal skeletal muscle. (A) Each line corresponds to the expression signal of each gene. Genes are ordered using the average linkage clustering method to group similar expression profiles. Red denotes up-regulated genes and green denotes down-regulated genes compared with adult control muscle. Note that the expression trends are almost identical within FCMD patients, and FCMD trends are distinct from those of normal children. (B) Expression profile of major muscle components of FCMD and DMD compared with that of normal children. Arrows show the relative expression change (single upward arrow and downward arrow, more than 2-fold increase/decrease; double upward arrows and downward arrows, more than 10-fold increase/decrease; rightward arrow, no change). Note that majority of muscle components are down-regulated in FCMD muscles.

Final maturation step is retarded in FCMD skeletal muscle

To investigate how differentiation is impaired, we examined histological specimens of FCMD skeletal muscle. Marked interstitial tissues with numerous small, round-shaped immature fibers and some necrotic fibers increased with age were seen in FCMD skeletal muscle specimens. Interstitial tissue is prominent from early infancy and progresses with age (Fig. 3A–C), and skeletal muscle from an FCMD fetus also shows rich interstitial tissues (Fig. 3E). Although necrotic change in muscle fibers is not so marked as in DMD fibers, DMD muscle shows less marked fibrosis and more mature fibers, despite more active necrotic and regenerating processes (Fig. 3D). Overall, FCMD muscle is reminiscent of fetal muscle; skeletal muscle from a normal fetus appears rich in fibrous tissues and small, round-shaped immature myotubes (Fig. 3F).

Muscle fiber type is easily identified by ATPase staining. Normally, type 2C fibers are mainly seen in fetal muscle fibers or in regenerating fibers. However, in ATPase-stained cryospecimens, FCMD muscle showed a significantly higher percentage of undifferentiated type 2C muscle fiber contents relative to DMD or control samples ($P < 0.005$) (Fig. 3G and H, Table 1).

Using immunohistochemical analysis, we examined MYH subtypes to confirm the differentiation impairment in FCMD and in myodystrophy mouse (*myd*), which is another model of secondary α-DGpathies. In normal muscle from age-matched controls, no staining of developmental or neonatal MYH (Fig. 3I and J) was seen. In contrast, FCMD and *myd* muscle fibers stained positively for developmental and neonatal MYHs (Fig. 3M and N). These positive fibers corresponded with those staining positive for fast-type MYHs in a serial section (Fig. 3M–O, arrows). Similar staining patterns were observed in skeletal muscle from an FCMD fetus. It is unlikely that all fibers showing developmental MYH expression are derived from regenerating fibers, as few active regenerating or necrotic fibers are seen in the hematoxylin and eosin (HE) specimen at any ages (Fig. 3A–C). Similar staining patterns were observed in skeletal muscles from an FCMD fetus and adult *myd* (data not shown). It is unlikely that all fibers showing developmental MYH expression are derived from regenerating fibers, as few active regenerating or necrotic fibers are seen in the HE specimen (Fig. 3A–C).

These results induce the possibility that maturation might be slowed or arrested in FCMD and *myd* skeletal muscles, and possibly this is common in secondary α-DGpathies. It also

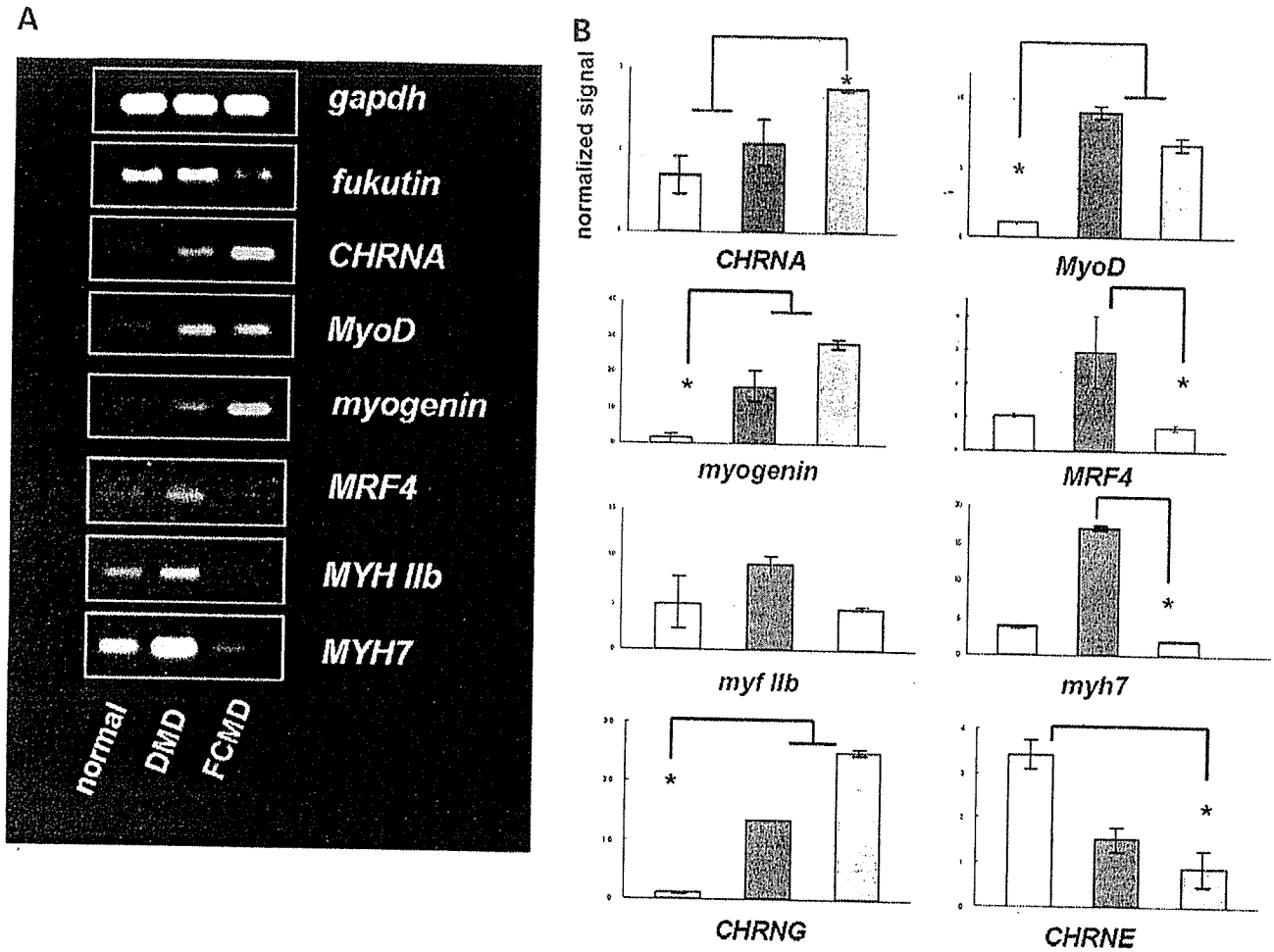

Figure 2. Differential expression of muscle components and myogenic factors in skeletal muscles from FCMD, DMD and normal children. (A) PCR products show that *MyoD* and *myogenin*, which are sequentially expressed in the early phase of muscle regeneration, are up-regulated in DMD and FCMD; however *MYH* and *MRF4* are down-regulated in FCMD but not DMD. (B) Quantitative real-time PCR analysis of mRNA expression. Each bar represents the mean value and 95% confidence interval of duplicate experiments in two patients for each disease and normal control. White bar, normal children; black bar, DMD; gray bar, FCMD. Expression levels are plotted as values normalized to *gapdh*. $^*P < 0.005$ (Student's *t*-test).

implies that secondary α-DGpathies have more complex etiology than the so-called 'muscular dystrophy', and that may be partly explained by a maturational defect.

NMJ abnormalities induce maturational delay in secondary α-DGpathies

Microarray analysis showed a reduction in *MRF4* expression in FCMD. Using immunochemistry, we further investigated MRF4 expression in FCMD and in *myd*. Immunoreactivity against MRF4 was reduced dramatically in FCMD muscle fibers (Fig. 4A). In normal skeletal muscles, anti-MRF4 antibody yielded strong signals, which co-localized with the nucleus and NMJs (Fig. 4A, upper columns). MRF4 in FCMD muscles showed weak signals which were not merged with NMJ (Fig. 4A, lower columns). Similar results were obtained in *myd* (data not shown). Regarding the fact that MRF4 is required at the time and place of NMJ development during skeletal muscle differentiation (23), these results prompt the hypothesis that the differentiation process of muscle fibers arrests at this point in secondary α-DGpathies.

We next examined the morphology of NMJs in both FCMD and *myd* by staining acetylcholine receptor (AchR) in NMJs with anti-α-bungarotoxin (Fig. 4B). Almost all the NMJs of FCMD and *myd* showed sparse, weak staining (Fig. 4B, lower columns), in contrast with the dense pattern in normal skeletal muscle (Fig. 4B, upper columns). In normal skeletal muscles, the borders of positive signals were characteristically flared because of multiple layers of synaptic folds, whereas borders in FCMD and *myd* appear smooth and simple, and synaptic folds—particularly secondary folds—were seldom observed. This signal pattern reflects deteriorated or non-deteriorated cluster of AChR on NMJs in secondary α-DGpathies.

Electron microscopic examination of these secondary α-DGpathies revealed aberrant NMJ lesions with abnormal neural endings. NMJs with fewer synaptic folds and secondary clefts were seen in all NMJs of FCMD and *myd* (Fig. 5A–F). In addition, the muscle fibers showed characteristics of immaturity, consistent with our hypothesis that the myotubes are maturationally arrested (Fig. 5G and H). These fibers are distinct from the active regenerating

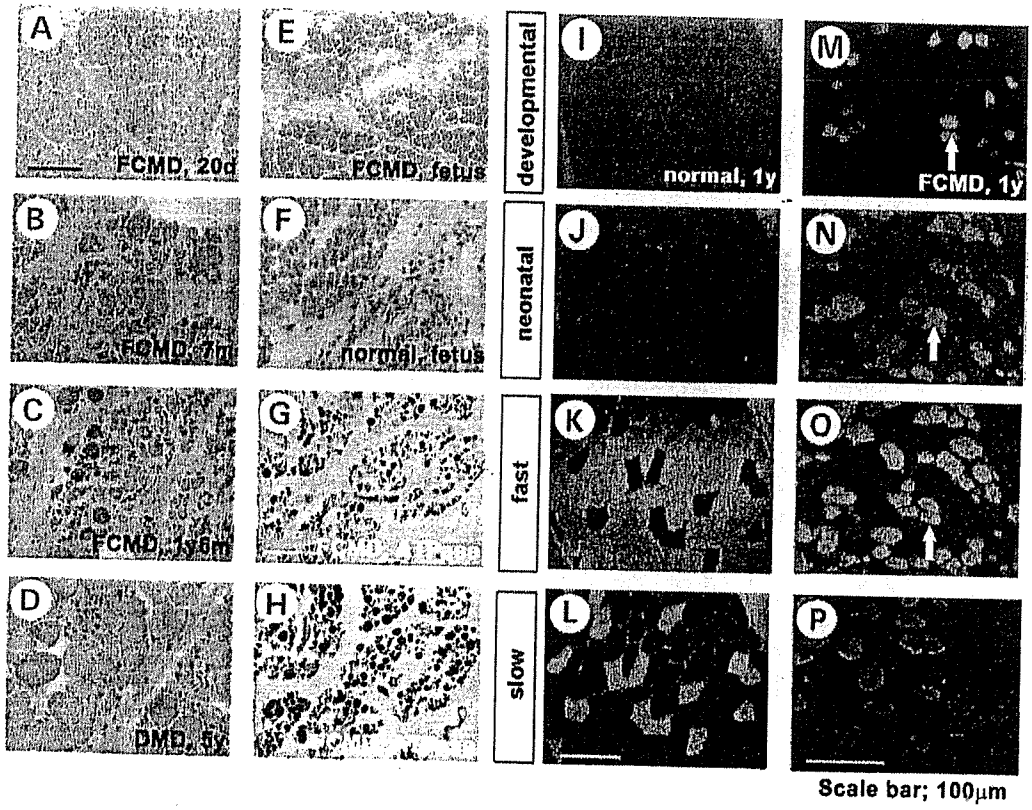

Figure 3. HE and ATPase stains of biopsied FCMD skeletal muscle, used for microarray analysis. Each specimen shows marked fibrosis with numerous small immature muscle fibers, which is seen from early infancy (A, 20 days; B, 7 months; C, 1-year 6 months), and progresses with age. DMD muscle (D, 5 years) shows less marked fibrosis and less frequent immature fibers despite more active necrotic and regenerating processes. Note that the pathological findings of FCMD skeletal muscles are similar to those of fetal skeletal muscles (E, FCMD fetus, 19 weeks; F, normal fetus, 21 weeks). Also note many undifferentiated immature type 2C fibers stained darkly for ATPase under both alkaline (pH 10.4) (G) and acid (pH 4.6) (H) pre-incubations. Immunostaining for MYH subtypes shows positive staining of developmental and neonatal MYH and decreased staining of slow-type MYH, which are distinct from normal muscles (normal child muscles, 1 year, I–L; FCMD, 1 year, M–P in sequential cryosections). Scale bars = 100 μm.

Table 1. Muscle contents and type 2C fibers in biopsied specimen of FCMD, DMD and normal children

Disease	Age	Muscle (%)	Type 2C (%)	Fibrosis (%)
FCMD (F1)	20 days	71	26	27
FCMD (F2)	7 months	53	26	41
FCMD (F3)	1-year 4 months	60	25	42
FCMD (F4)	1-year 6 months	52	19	43
DMD[a]	3–9 years	61	9	30
Normal[a]	1 year	≥95	≤5	≤5

[a]Average, $n = 10$

myotubes seen in DMD muscle fibers, in that ribosome particles appear quite poor.

We performed functional analysis of the morphologically aberrant NMJs in secondary α-DGpathy by measuring miniature endplate potential (MEPP) and endplate potential (EPP) of *myd* mice (Table 2). The amplitudes of MEPP were markedly lower in *myd* mice than in normal littermates ($P < 0.005$). In contrast, quantal content of EPP was increased in *myd* ($P < 0.005$). The reduction of MEPP amplitude could be compensated by the increased quantal content, and the safety margin of neuromuscular transmission is considered to be maintained in *myd* mice. The number of endplates recorded in *myd* mice was much fewer than in normal littermates. However, the amount of *d*-Tubocurarine that can inhibit the muscle contraction induced by the EPP was distinctively low for *myd* muscle relative to that of normal littermate (Table 2). These findings implicate, combined with the morphological observation, that most of the endplates in *myd* are not adequately innervated, but a small number of NMJs functionally compensate the low MEPP amplitude to maintain the safety margin of neuromuscular transmission.

Hypoglycosylation of α-DG as the etiology of non-clustering AChR in NMJs

We performed immunostaining to examine core α-DG in muscle fibers. In normal skeletal muscles, α-DG localized to the NMJ and sarcoplasmic membrane (Fig. 6A). In contrast, FCMD and *myd* showed substantial α-DG on the sarcoplasmic membrane, but only weak signals were observed in thin NMJs, indicating a failure of α-DG aggregation (Fig. 6A, normal NMJs, arrows; FCMD and *myd*, arrowheads). We also examined staining of glycosylated α-DG (IIH6). As expected, we saw no signal on NMJs or on the sarcoplasmic membrane in FCMD and *myd* (data not shown), implying that glycosylation

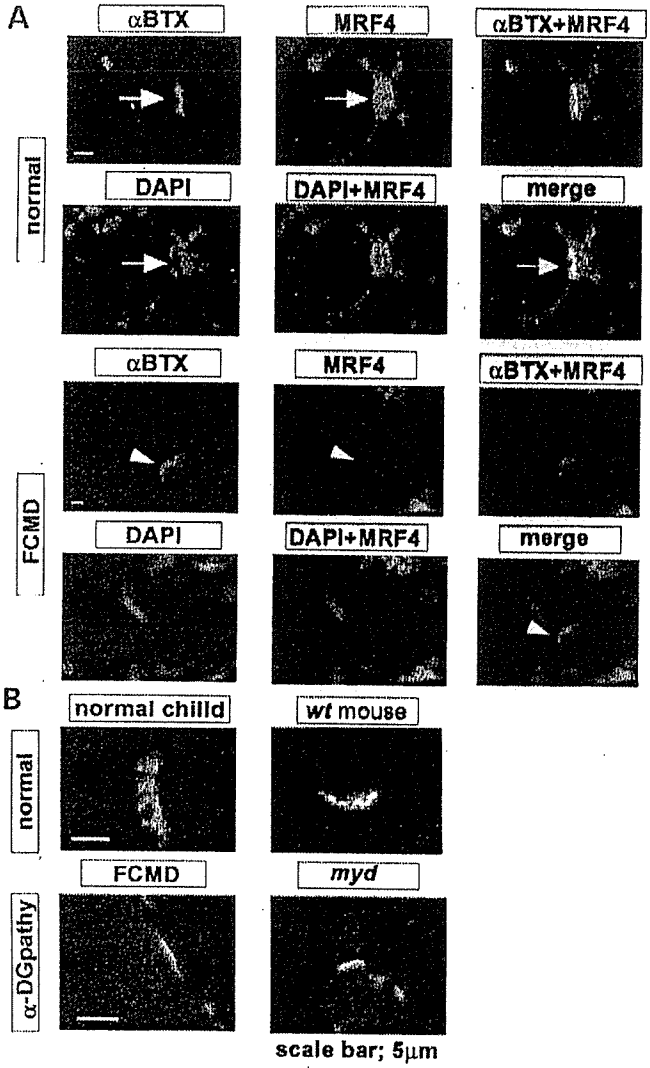

Figure 4. Immunohistochemistry of MRF4 in secondary α-DGpathy and aberrant NMJs in secondary α-DGpathy. (A) Fluorescence image of MRF4 (green), α-bungarotoxin staining of AChR on NMJ (red) and DAPI-stained nuclei (blue) in normal and FCMD skeletal muscles. In normal muscle, NMJs stain strongly, merging with MRF4 staining and DAPI (arrows, upper columns). In FCMD, the staining pattern of MRF4 in the nucleus of muscle fibers is markedly decreased and no merging stain with NMJ is seen (arrowhead). (B) Compared with normal AChR on NMJs (red) stained by α-BTX (upper columns), scattered, fold-less staining pattern is present in both FCMD and *myd* (lower columns). Scale bars = 5 μm.

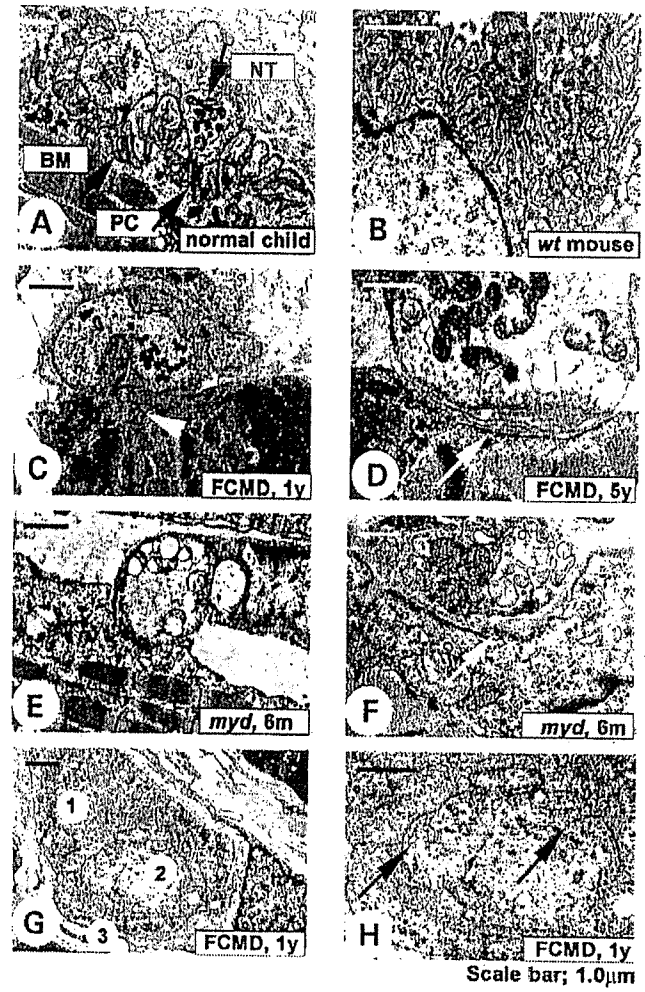

Figure 5. Electron microscopic examinations of NMJs and skeletal muscle from secondary α-DGpathies. Aberrant NMJs and myotubes with maturational arrest are seen in secondary α-DGpathies. Compared with normal (A, human; B, *wt* mouse), NMJs in FCMD (C and D) and *myd* (E and F) show simpler secondary clefts and wider synaptic clefts with occasional multilayered basal lamina (D and F, white arrows). Moreover, maturationally arrested myotubes are seen in secondary α-DGpathy. Three cells (1–3) share a common basement membrane (G), and at higher magnification, these myotubes contain poorly organized myofibrils (black arrows) (H). In contrast with early regenerating fibers in normal regenerating myotubes, ribosome particles are not abundant in FCMD, indicating maturational arrest of myotubes in secondary α-DGpathy. Abbreviation: PC, primary cleft; NT, nerve terminal; BM, basal lamina. Scale bars = 1.0 μm.

is crucial for α-DG aggregation and also for the subsequent clustering of AChR in NMJs. α-DG is expressed on both the muscle peripheral membrane and the peripheral nerve terminal at NMJs (24). Thus, we examined whether a pre-synaptic or post-synaptic lesion contributes to aberrant NMJ formation. Staining for synaptophysin at the pre-synaptic region or for fasciculin at the synaptic gap showed abnormal patterns similar to that of α-bungarotoxin (Fig. 6B). These observations indicate that NMJ abnormalities in secondary α-DGpathies may arise not only at the post-synaptic muscle peripheral membrane, but also by pre-synaptic hypoglycosylated α-DG.

Utrophin and dystrophin are expressed abundantly in pre- and post-synaptic regions of mature NMJs and suggested to play an important role for synaptic maturation and the maintenance of NMJs (25). To analyze aberrations of the distribution of utrophin and dystrophin, we performed immunostaining for utrophin and dystrophin in NMJs. Examination under confocal microscopy allowed a precise view of both proteins on the sarcoplasmic membrane. In NMJs from a normal sample, utrophin strongly stains exclusively at fine primary and secondary synaptic folds, tangled with dystrophin staining just beneath the muscle peripheral membrane (Fig. 6C, left column; Fig. 6D, upper columns). In contrast, NMJs from secondary α-DGpathies show thinner, fold-less and weak signals for both utrophin and dystrophin (Fig. 6C, right column; Fig. 6D, middle and lower

Table 2. Functional analysis of NMJs in *myd* mice

	MEPP amplitude (mV)[a]	Quantal content (*m*)[a]	*d*-Tubocurarine concentration (μg/ml)[b]
Control 1	0.52 ± 0.07 (n = 16)	49.1 ± 5.5 (n = 10)	0.38
Control 2	0.64 ± 0.10 (n = 18)	52.8 ± 3.8 (n = 14)	0.45
myd 1	0.32 ± 0.04 (n = 11)	65.6 ± 6.5 (n = 5)	0.30
myd 2	0.36 ± 0.06 (n = 7)	75.4 ± 38.7 (n = 5)	0.30

[a]Values given are mean ± SEM and number of endplates (in parentheses).
[b]The amount of *d*-Tubocurarine that can inhibit the muscle contraction induced by the EPP.

columns). The utrophin signal was exclusively seen on NMJs, but weakly seen on muscle sarcoplasmic membrane in FCMD (Fig. 6C, right column), which is usually seen in regenerating muscle fibers (26). NMJs from fetal wild-type or *myd* showed similar staining patterns as expected (data not shown), suggesting that this staining pattern is indicative of immature muscle fibers. This observation is consistent with our hypothesis that NMJ formation in secondary α-DGpathies is developmentally arrested during myotube maturation in the fetal phase.

DISCUSSION

FCMD has long been classified as 'muscular dystrophy', although the clinical characteristics differ from those of DMD. Muscular dystrophy is defined generally by necrotic change and active regeneration of muscle fibers. However, FCMD muscle in infantile stage seems more likely to have additional features, implying a more complex pathogenesis for FCMD. Indeed, our microarray analysis showed that general expression profiling clusters FCMD and DMD distinctively. Expression of mature muscle components was surprisingly low in FCMD, indicating less active regeneration of muscle fibers. We also saw similar expression profiles among all FCMD patients in our samples, indicating that FCMD is a chronic rather than progressive disorder, at least at the infantile period.

We confirmed maturational delay and aberrant NMJs in FCMD skeletal muscle fibers by expression profiling, morphological and histochemical analysis, and electrophysiological examination. These findings are common to secondary α-DGpathies but are not seen in DMD. In this study, we demonstrate that the etiology of secondary α-DGpathy skeletal muscle abnormalities may stem from maturational arrest caused by aberrant NMJs in addition to dystrophy. MDC1A, clinical characteristics of which are similar to FCMD, is described with an initial phase of necrosis and regeneration in the early steps of the disease (6). Although aberrant NMJ is also seen in MDC1A (27), the muscle fragility due to defect in the component of basement membrane mainly affects the phenotype and causes necrosis and regeneration.

A considerable body of evidence indicates that muscle differentiation ceases at NMJ formation in FCMD. First, immature type 2C fibers are predominant in FCMD (Table 1). At the initiation of muscle differentiation, satellite cells proliferate to become myoblasts, fuse to organize myotubes. These early myotubes contain type 2C fibers. Following NMJ formation, immature fibers are induced to differentiate further into mature muscle fibers such as type 1, 2A and 2B. Second, down-regulated expression of matured MYHs in FCMD also suggests arrest at this stage. Following completion of NMJ formation, embryonic, neonatal-type MYHs in immature myofibers are replaced by adult-type, slow MYHs, which are induced by extracellular matrix (ECM) components, growth factors or programmed cell differentiation (28).

Third, MRF4, which is postulated to be induced by AChR clustering in NMJ formation, is down-regulated in FCMD. Normally, during the early phase of muscle development, a series of myogenic regulatory genes such as *myf5*, *MyoD* and *myogenin* are sequentially expressed, followed by MRF4 up-regulation just after NMJ formation. AChRs bind to myotubes, associate with specific factors and trigger a signal to induce expression of myogenic factors including MRF4, which is suggested to play a crucial role in muscle terminal maturation and maintenance (20,21,29). Therefore, MRF4 is distinct from MyoD, myogenin and myf5 in that it is expressed mainly in matured myotubes and myofibers. MRF4 has been reported to co-localize with AChR in NMJs and to function in terminal muscle maturation and fiber maintenance (30). It is reasonable to assume that MRF4 function is required at the time and place of NMJ development during skeletal muscle differentiation (23). These results prompt the hypothesis that the differentiation process of muscle fibers arrests at this point in FCMD and *myd*.

Fourth, the fact that high *CHRNG* and low *CHRNE* expression in FCMD muscle relative to that in age-matched normal control or DMD muscle is striking, although the age of the DMD patient was slightly higher than that of the FCMD patients. It clearly indicates that most of the AChR in FCMD muscle is fetal type. It also supports our hypothesis that skeletal muscle in secondary α-DGpathy is immature and that delay of differentiation might be involved with maturation defect of NMJs.

What causes aberrant NMJs in secondary α-DGpathies? Normally, NMJs are built by a dense tangle of sarcoplasmic membrane and neural endings through a layer of basement membrane. It is possible that connections between the neural terminal and glycosylated α-DG, made through a layer of basement membrane and mediated by molecules such as laminin or agrin, are important to normal NMJ formation and subsequent muscle differentiation (31,32). MDC1A, clinical characteristics of which are similar to FCMD (6), also shows aberrant NMJs with fewer synaptic folds (27). In contrast, Musk or rapsyn deficiency does not resemble severe muscular dystrophy in spite of the abnormal NMJ formation. The interaction of laminin and α-DG is thought to play an essential role in the transition of AChR microaggregates into macroaggregates at the developing NMJ, followed by the concentration of α-DG on NMJs (32,33). These facts lend support to our hypothesis that the laminin/α-DG interaction fulfills a pivotal function in normal NMJ formation.

Alternatively, it is also possible that attachment of neural terminals to NMJs is affected pre-synaptically in secondary α-DGpathies. Abnormalities in the pre-synaptic peripheral nerve would affect the neural endings of NMJs, leading to

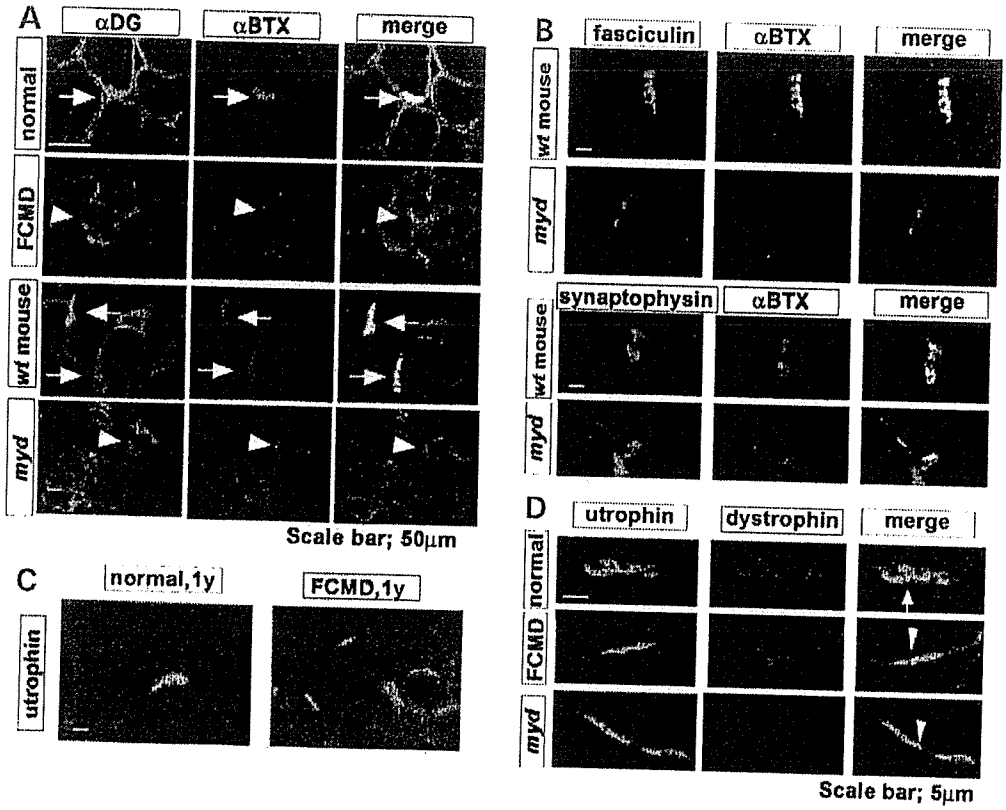

Figure 6. Aberrant NMJs and lack of α-dystroglycan aggregation in NMJs affect pre- and post-synaptic formation of NMJs in secondary α-DGpathy. (A) α-DG (green) strongly co-localizes with α-BTX in NMJs of normal skeletal muscle, merged yellow (arrows). However in secondary α-DGpathies, the lack of α-dystroglycan aggregation on aberrant formed NMJs is seen despite positive staining on muscle peripheral membrane, as evidenced by the lack of co-localization signal in merged columns (arrowheads). (B) Green-stained pre-synaptic markers (fasciculin, AChE marker; synaptophysin, pre-synaptic vesicle marker) also show the aberrant staining pattern of NMJs, shown in merged staining with α-BTX (red) in *myd*. (C) Utrophin remains on sarcoplasmic membrane on secondary α-DGpathies. Although green-stained utrophin aggregates exclusively on NMJs of normal muscle fibers, utrophin remains on sarcoplasmic membrane of FCMD muscle fibers. (D) Confocal imaging of utrophin and dystrophin on NMJs of secondary α-DGpathy. Merged column in normal NMJs (arrow) shows that fine primary and secondary folds lined with utrophin are tangled with dystrophin staining on NMJs, which also line the peripheral membrane of muscle fibers. Note that in secondary α-DGpathies, secondary folds are severely lacking (arrowheads). Thin, scattered utrophin staining and markedly decreased staining of dystrophin on NMJs are seen in both FCMD and *myd*. Scale bars = 5 μm.

deficient differentiation signal transduction to FCMD muscle fibers and arrested post-synaptic muscle differentiation. It has been suggested that α-DG in the central or peripheral nervous system is hypoglycosylated in secondary α-DGpathies (34). *O*-Mannose-type glycoprotein is suggested to contribute to the stability and maintenance of muscle cell membrane, synaptic formation and myelination of peripheral nerves, although the precise mechanism of α-DG activity in peripheral nerve tissue is unclear. The dystrophin–glycoprotein complex on Schwann cells is also thought to be important in peripheral myelinogenesis, regeneration, differentiation, apoptosis and polarity of skeletal muscle cells (35). Although Ishii *et al.* (36) reported that electron microscopy of Schwann cells on FCMD muscle revealed no pathologic findings, neural transmission may be developmentally impaired and collapsed as a result of hypoglycosylated α-DG.

Naturally, our data do not rule out the other possibilities for immaturity of the skeletal muscles of α-DGpathies. Although the expression profile and histochemical data indicate that skeletal muscles are in a persistent undifferentiated state, it is possible that the regeneration process fulfills a crucial function in the phenomenon observed in skeletal muscles of α-DGpathies. It is also possible that most of the muscle fibers are under denervation status, because motor neurons are unable to maintain strong attachments to myofibers, leading to a constant stimulation of denervation signal pathways. Although we demonstrated substantial evidences for the aberrant NMJ, the pathogenesis of skeletal muscles in α-DGpathies is likely to be a combination of these problems and of multifactorial origin.

Taken together, these findings show that muscle fibers in secondary α-DGpathies are developmentally arrested more to 'dystrophic', perhaps because hypoglycosylated α-DG precludes proper aggregation on NMJs, preventing AChR clustering. These defects may disrupt terminal muscle maturation, which is induced after innervation of neurons on the muscle peripheral membrane via a basement membrane layer. Dystrophic changes traditionally thought to underlie 'muscular dystrophy' are caused by attenuated physical connections between α-DG and the muscle basement membrane. We propose that the muscle lesion in secondary α-DGpathies is caused by complex pathogenesis, not only by dystrophic change but more importantly, maturational arrest resulting from chronically delayed terminal muscle fiber maturation and NMJ deficiency. To date, no clinical approaches to secondary α-DGpathies exist. These findings open a possible

avenue for treating muscle tissues in these congenital muscular dystrophies, via targeted induction of NMJ maturation in muscle fibers.

MATERIALS AND METHODS

Samples

All clinical materials were collected for diagnostic purposes. Four muscle specimens (biceps branchii) from FCMD patients (ages: 20 days, 7 months, 1-year 4 months, and 1-year 6 months) were used in the analysis. Genetic screening identified a homozygous retrotransposal insertion into the 3′ untranslated region of *fukutin* in all FCMD patients (3). For the non-dystrophic muscle controls, muscle RNAs from two children (ages: 1 year) was used. These patients were selected based on normal laboratory findings, normal plasma CK levels and no histopathological evidence for muscular dystrophy.

We also obtained myodystrophy (Large^{myd}) mice and control littermates (Large$^{myd/+}$ or Large$^{+/+}$), aged 3 and 6 months, by mating heterozygous pairs provided by Jackson Laboratories.

RNA isolation and expression profiling

Generation of cDNA microarrays containing skeletal muscle transcripts has been reported previously (19). Using similar methods, we constructed a new cDNA chip containing 5600 genes expressed in skeletal muscle. RNA isolation, hybridization and detection methods also have been reported previously. Microarray experiments were carried out using a competitive hybridization method with two labeled targets: one for muscle RNAs from FCMD patients or normal children, and another for pooled muscle RNAs (Origene), which served as a template control for per-chip normalization. Each analysis was conducted at least twice. The hybridization intensities of each spot and the background intensities were calculated using a ScanArray 5000 microarray scanner with Quant Array software (Perkin-Elmer Life Science).

Microarray data analysis

Analysis of microarray data was performed using Genespring version 6.1 (Silicon Genetics) software. Data used for further analysis were calculated using a previously reported method (19). To avoid 'false-positive' signals, we excluded genes from the analysis for which average normal expression level constraints are under 500. We sorted 1790 genes from a total of 5600 for further analysis.

Quantitative real-time PCR

Two patients with FCMD (ages: 10 months and 1 year), two patients with DMD (ages: 1 and 7 years) and two normal children (ages: 1 and 2 years) were used for quantitative RT-PCR using skeletal muscle RNAs. Single-strand cDNA was produced with random primers, and quantitative real-time RT-PCR using SYBR-green was performed using the ABI Prism 7900 sequence detection system (Applied Biosynthesis). Data analysis was performed in duplicate experiments. Statistical significance was evaluated using Student's *t*-test, and $P < 0.05$ was considered significant. The primers used for the experiments are shown in Supplementary Material, Table S1. *Gapdh* was used as an internal control.

Imaging analysis

HE staining and ATPase staining were performed on cryosections. ATPase staining was performed at pH 9.4–10.6 and 4.2–4.6. For ATPase staining, average data from 10 DMD patients (ages: 3–9) and 10 normal control cases (ages: around 1 year) were selected. Scion Image Beta 3b (Scion Corporation) was used for estimating the content of type 2C fibers, muscle fibers, adipose tissues and interstitial tissues (Table 1). Statistical analysis was performed using Student's *t*-test.

Immunohistochemistry

All muscle specimens were processed for cryosectioning (8-μm thick) and fixed in 50% ethanol and 50% acetic acid for 1 min. Anti-core α-dystroglycan [GT20ADG, gift from Dr Kevin Campbell (5)], rhodamine-conjugated α-bungarotoxin (BTX, Molecular Probes), anti-synaptophysin (NCL-SYNAPp, Novocastra), Alexa-fluor488 labeled anti-fasciculin2 (F4293, Sigma), anti-MRF4 (C-19, Cruz Biotechnology), anti-utrophin (UT2, gift from Dr Michihiro Imamura), anti-human dystrophin (NCL-DYS2, Novocastra), anti-human dystrophin (MANDRA-1, Sigma) and anti-myosin heavy chain for developmental, neonatal, fast and slow types (NCL-MHCd, MHCn, MHCf and MHCs, respectively, Novocastra) were used to stain NMJs.

Electron microscopy

Muscle specimens were obtained from four patients diagnosed as FCMD (ages: 6 months to 4 years old) and from two normal children (ages: 1 year). Five NMJs were found in three FCMD patients' skeletal muscle and four normal NMJs were examined in two normal children. Intercostal muscles and soleus muscles were dissected from myodystrophy and control mice, and cut into 1-mm thick cubes. Four NMJs were examined in myd and normal controls, respectively. Samples were fixed in 2% glutaraldehyde and embedded in epoxy resin as described previously (36). Ultrathin (50–90-nm thick) sections were cut on an Ultracut S ultramicrotome (Reichert).

Electrophysiologic examination

Diaphragms with its motor nerve were dissected and used for the conventional intracellular microelectrode study (37). MEPPs, EPPs and resting membrane potentials (RMPs) were recorded. For EPP recording, the phrenic nerve was stimulated using a suction electrode at 0.5 Hz. *d*-Tubocurarine chloride (Curaren, Sigma) was used at a concentration sufficient to inhibit muscle contraction. The potentials were corrected for non-linear summation and the last 64 responses in a train of 114 were saved for later analysis. The quantal content *m* was calculated by the variance method. MEPP and EPP amplitudes were corrected to a standard RMP of −80 mV. To correct MEPP amplitude by the fiber diameter, the geometric

mean of the shortest and longest diameters of muscle fibers was determined in 30 randomly selected muscle fibers in cryostat sections.

SUPPLEMENTARY MATERIAL

Supplementary Material is available at HMG Online.

ACKNOWLEDGEMENTS

We are grateful to Drs Fumiaki Saito and Shin'ichi Takeda for their critical comments, Fumie Uematsu and Eiji Oiki for technical support and Dr Jennifer Logan for editing the manuscript. This work was supported by a Health Science Research Grant, Research on Psychiatric and Neurological Diseases and Mental Health, from the Ministry of Health, Labor, and Welfare of Japan; and by the 21st Century COE program from the Ministry of Education, Culture, Sports, Science, and Technology of Japan.

Conflict of Interest statement. None declared.

REFERENCES

1 Fukuyama, Y., Osawa, M. and Suzuki, H. (1981) Congenital progressive muscular dystrophy of the Fukuyama type—clinical, genetic and pathological considerations. *Brain Dev.*, **3**, 1–29.
2. Toda, T., Segawa, M., Nomura, Y., Nonaka, I., Masuda, K., Ishihara, T., Sakai, M., Tomita, I., Origuchi, Y., Suzuki, M. *et al.* (1993) Localization of a gene for Fukuyama type congenital muscular dystrophy to chromosome 9q31–33. *Nat. Genet.*, **5**, 283–286.
3. Kobayashi, K., Nakahori, Y., Miyake, M., Matsumura, K., Kondo-Iida, E., Nomura, Y., Segawa, M., Yoshioka, M., Saito, K., Osawa, M. *et al.* (1998) An ancient retrotransposal insertion causes Fukuyama-type congenital muscular dystrophy. *Nature*, **394**, 388–392.
4 Hayashi, Y.K., Ogawa, M., Tagawa, K., Noguchi, S., Ishihara, T., Nonaka, I. and Arahata, K. (2001) Selective deficiency of alpha-dystroglycan in Fukuyama-type congenital muscular dystrophy. *Neurology*, **57**, 115–121.
5 Michele, D.E., Barresi, R., Kanagawa, M., Saito, F., Cohn, R.D., Satz, J.S., Dollar, J., Nishino, I., Kelley, R.I., Somer, H. *et al.* (2002) Post-translational disruption of dystroglycan–ligand interactions in congenital muscular dystrophies. *Nature*, **418**, 417–422.
6 Tome, F.M., Evangelista, T., Leclerc, A., Sunada, Y., Manole, E., Estournet, B., Barois, A., Campbell, K.P. and Fardeau, M. (1994) Congenital muscular dystrophy with merosin deficiency. *C R Acad Sci III*, **317**, 351–357.
7 Muntoni, F., Brockington, M., Blake, D.J., Torelli, S. and Brown, S.C. (2002) Defective glycosylation in muscular dystrophy. *Lancet*, **360**, 1419–1421.
8. Hohenester, E., Tisi, D., Talts, J.F. and Timpl, R. (1999) The crystal structure of a laminin G-like module reveals the molecular basis of alpha-dystroglycan binding to laminins, perlecan, and agrin. *Mol. Cell*, **4**, 783–792.
9 Yoshida, A., Kobayashi, K., Manya, H., Taniguchi, K., Kano, H., Mizuno, M., Inazu, T., Mitsuhashi, H., Takahashi, S., Takeuchi, M. *et al.* (2001) Muscular dystrophy and neuronal migration disorder caused by mutations in a glycosyltransferase, POMGnT1. *Dev. Cell.*, **1**, 717–724.
10 Beltran-Valero de Bernabe, D., Currier, S., Steinbrecher, A., Celli, J., van Beusekom, E., van der Zwaag, B., Kayserili, H., Merlini, L., Chitayat, D., Dobyns, W.B. *et al.* (2002) Mutations in the *O*-mannosyltransferase gene POMT1 give rise to the severe neuronal migration disorder Walker–Warburg syndrome. *Am. J. Hum. Genet.*, **71**, 1033–1043.
11 van Reeuwijk, J., Janssen, M., van den Elzen, C., Beltran-Valero de Bernabe, D., Sabatelli, P., Merlini, L., Boon, M., Scheffer, H., Brockington, M., Muntoni, F. *et al.* (2005) POMT2 mutations cause alpha-dystroglycan hypoglycosylation and Walker–Warburg syndrome. *J. Med. Genet.*, **12**, 907–912.
12 Brockington, M., Yuva, Y., Prandini, P., Brown, S.C., Torelli, S., Benson, M.A., Herrmann, R., Anderson, L.V., Bashir, R., Burgunder, J.M. *et al.* (2001) Mutations in the fukutin-related protein gene (FKRP) identify limb girdle muscular dystrophy 2I as a milder allelic variant of congenital muscular dystrophy MDC1C. *Hum. Mol. Genet.*, **10**, 2851–2859.
13. Grewal, P.K., Holzfeind, P.J., Bittner, R.E. and Hewitt, J.E. (2001) Mutant glycosyltransferase and altered glycosylation of alpha-dystroglycan in the myodystrophy mouse. *Nat. Genet.*, **28**, 151–154.
14. Longman, C., Brockington, M., Torelli, S., Jimenez-Mallebrera, C., Kennedy, C., Khalil, N., Feng, L., Saran, R.K., Voit, T., Merlini, L. *et al.* (2003) Mutations in the human LARGE gene cause MDC1D, a novel form of congenital muscular dystrophy with severe mental retardation and abnormal glycosylation of alpha-dystroglycan. *Hum. Mol. Genet.*, **12**, 2853–2861.
15. Nonaka, I., Sugita, H., Takada, K. and Kumagai, K. (1982) Muscle histochemistry in congenital muscular dystrophy with central nervous system involvement. *Muscle Nerve*, **5**, 102–106.
16. Terasawa, K. (1986) Muscle regeneration and satellite cells in Fukuyama type congenital muscular dystrophy. *Muscle Nerve*, **5**, 465–470.
17. Chen, Y.W., Zhao, P., Borup, R. and Hoffman, E.P. (2000) Expression profiling in the muscular dystrophies: identification of novel aspects of molecular pathophysiology. *J. Cell Biol.*, **151**, 1321–1336.
18. Haslett, J.N., Sanoudou, D., Kho, A.T., Bennett, R.R., Greenberg, S.A., Kohane, I.S., Beggs, A.H. and Kunkel, L.M. (2002) Gene expression comparison of biopsies from Duchenne muscular dystrophy (DMD) and normal skeletal muscle. *Proc. Natl Acad. Sci. USA*, **99**, 15000–15005.
19. Noguchi, S., Tsukahara, T., Fujita, M., Kurokawa, R., Tachikawa, M., Toda, T., Tsujimoto, A., Arahata, K. and Nishino, I. (2003) cDNA microarray analysis of individual Duchenne muscular dystrophy patients. *Hum. Mol. Genet.*, **12**, 595–600.
20 Prody, C.A. and Merlie, J.P. (1991) A developmental and tissue-specific enhancer in the mouse skeletal muscle acetylcholine receptor alpha-subunit gene regulated by myogenic factors. *J. Biol. Chem.*, **266**, 22588–22596.
21 Fujisawa-Sehara, A., Nabeshima, Y., Komiya, T., Uetsuki, T., Asakura, A. and Nabeshima, Y. (1992) Differential *trans*-activation of muscle-specific regulatory elements including the myosin light chain box by chicken MyoD, myogenin, and MRF4. *J. Biol. Chem.*, **267**, 10031–10038.
22. Mishina, M., Takai, T., Imoto, K., Noda, M., Takahashi, T., Numa, S., Methfessel, C. and Sakmann, B. (1986) Molecular distinction between fetal and adult forms of muscle acetylcholine receptor. *Nature*, **321**, 406–411.
23. Sunyer, T. and Merlie, J.P. (1993) Cell type- and differentiation-dependent expression from the mouse acetylcholine receptor epsilon-subunit promoter. *J. Neurosci. Res.*, **36**, 224–234.
24 Jacinthe, G. and Michael, F. (2001) Expression and localization of agrin during sympathetic synapse formation *in vitro*. *J. Neurobiol.*, **48**, 228–242.
25. Grady, R.M., Zhou, H., Cunningham, J.M., Henry, M.D., Campbell, K.P. and Sanes, J.R. (2000) Maturation and maintenance of the neuromuscular synapse: genetic evidence for roles of the dystrophin–glycoprotein complex. *Neuron*, **25**, 279–293.
26 Helliwell, T.R., Man, N.T., Morris, G.E. and Davies, K.E. (1992) The dystrophin-related protein, utrophin, is expressed on the sarcolemma of regenerating human skeletal muscle fibres in dystrophies and inflammatory myopathies. *Neuromuscul. Disord.*, **3**, 177–184.
27. Noakes, P.G., Gautam, M., Mudd, J., Sanes, J.R. and Merlie, J.P. (1995) Aberrant differentiation of neuromuscular junctions in mice lacking s-laminin/laminin beta 2. *Nature*, **374**, 258–262.
28. Miller, J.B. and Stockdale, F.E. (1986) Developmental origins of skeletal muscle fibers: clonal analysis of myogenic cell lineages based on expression of fast and slow myosin heavy chains. *Proc. Natl Acad. Sci. USA*, **83**, 3860–3864.